

RESEARCH ARTICLE

Alkaline guts contribute to immunity during exposure to acidified seawater in the sea urchin larva

Meike Stumpp^{1,*}, Inga Petersen², Femke Thoben¹, Jia-Jiun Yan³, Matthias Leippe¹ and Marian Y. Hu^{2,*}

ABSTRACT

Larval stages of members of the Ambulacraria superphylum including echinoderms and hemichordates have highly alkaline midguts. To date, the reason for the evolution of such extreme pH conditions in the gut of these organisms remains unknown. Here, we test the hypothesis that, analogous to the acidic stomachs of vertebrates, these alkaline conditions may represent a first defensive barrier to protect from environmental pathogens. pH-optimum curves for five different species of marine bacteria demonstrated a rapid decrease in proliferation rates by 50–60% between pH 8.5 and 9.5. Using the marine bacterium *Vibrio diazotrophicus*, which elicits a coordinated immune response in the larvae of the sea urchin *Strongylocentrotus purpuratus*, we studied the physiological responses of the midgut pH regulatory machinery to this pathogen. Gastroscopic microelectrode measurements demonstrate a stimulation of midgut alkalization upon infection with *V. diazotrophicus* accompanied by an upregulation of acid–base transporter transcripts of the midgut. Pharmacological inhibition of midgut alkalization resulted in an increased mortality rate of larvae during *Vibrio* infection. Reductions in seawater pH resembling ocean acidification conditions lead to moderate reductions in midgut alkalization. However, these reductions in midgut pH do not affect the immune response or resilience of sea urchin larvae to a *Vibrio* infection under ocean acidification conditions. Our study addressed the evolutionary benefits of the alkaline midgut of Ambulacraria larval stages. The data indicate that alkaline conditions in the gut may serve as a first defensive barrier against environmental pathogens and that this mechanism can compensate for changes in seawater pH.

KEY WORDS: *Vibrio diazotrophicus*, Ocean acidification, Bacterial infection, Na⁺/H⁺-exchange, Ion selective micro-electrodes

INTRODUCTION

Distinct regulation of gastro-intestinal pH is a requisite for homeostasis in most metazoans. In particular, an acidic gastric pH is found in vertebrates including humans and serves as the primary innate defense against environmental pathogens in the gastro-intestinal tract (Koelz, 1992; Tennant et al., 2008; Beasley et al., 2015). Here, bacterial infections and inflammations are often associated with dysfunction of gastric pH regulation (Jaskiewicz et al., 1990; Smith, 2003; Beasley et al., 2015). Highly alkaline

conditions (pH > 11) were described in the guts of insects including lepidopteran and dipteran larvae as well as some termite species (Azuma et al., 1995; Brune and Kühl, 1996; Boudko et al., 2001). In termites, highly alkaline conditions up to pH 12 are found in the midgut–hindgut junctions and serve to maintain a specific gut microbiome that aids the digestion and fermentation of cellulose-rich diets (Brune and Kühl, 1996; Brune, 1998). In contrast, microbiome studies on lepidopteran larvae indicate that the highly alkaline caterpillar gut contains a low amount of microbial residents and does not reveal a specific composition of the gut microbial communities (e.g. Hammer et al., 2017). It has been speculated that owing to the extreme pH conditions and the simple morphology, designed for rapid digestive throughput, microbes cannot persist in the caterpillar gut (Hammer et al., 2017). Accordingly, distinct pH environments in the guts of metazoans appear to have evolved to serve different feeding strategies and to control the microbial composition of the gut.

The larval stages of echinoderms and hemichordates have been demonstrated to also display highly alkaline conditions in their midguts ranging from pH 8.5 to 10.5 (Stumpp et al., 2013, 2015; Hu et al., 2017). The current model denotes that this alkalization of the midgut is generated by acid–base transporters, including primary active ion pumps, i.e. Na⁺/K⁺-ATPase and V-type H⁺ATPase, and secondary active transporters, i.e. Na⁺/H⁺-exchangers and HCO₃[−] transporters (Stumpp et al., 2015). Although differences in the alkalization mechanism were described for echinoderm and hemichordate larvae, maintenance of an alkaline midgut in both phyla is strongly dependent on Na⁺/H⁺-exchange activity (Stumpp et al., 2015). Accordingly, maintenance of an alkaline midgut during exposure to acidified seawater has been hypothesized to be a major factor affecting the larval energy budget explaining reduced developmental rates under simulated ocean acidification (OA) (Stumpp et al., 2011, 2013; Pan et al., 2015; Lee et al., 2019). In addition, determination of digestive enzyme activities in combination with *in vivo* feeding rates demonstrated reduced ability to digest algae during exposure to reductions in seawater pH in the context of OA. This reduction in feeding rates was accompanied by a partly compensated reduction in midgut pH under OA conditions (Stumpp et al., 2013; Lee et al., 2019). It was concluded that reduced developmental rates of echinoderm and hemichordate larval stages can be attributed to reduced digestion efficiencies as well as increased energetic costs to, at least partly, maintain midgut pH (Stumpp et al., 2011; Pan et al., 2015; Lee et al., 2019). A multi-species comparison suggested that the regulatory efforts to maintain alkaline conditions in the guts of brittlestars, sea stars, sea urchins and hemichordates are a key trait determining the sensitivity of these species to OA (Hu et al., 2017). Despite the knowledge about the existence of alkaline guts in Ambulacraria larvae and their response to OA, it remains enigmatic why these extraordinary conditions evolved in the digestive tracts of these animals.

¹Zoological Institute, Christian-Albrechts University of Kiel, 24118 Kiel, Germany.

²Institute of Physiology, Christian-Albrechts University of Kiel, 24118 Kiel, Germany.

³Institute of Cellular and Organismic Biology, Academia Sinica, 115, Taipei, Taiwan.

*Authors for correspondence (m.hu@physiologie.uni-kiel.de; mstumpp@zoologie.uni-kiel.de)

© M.S., 0000-0001-7765-2996; F.T., 0000-0003-0814-5442; M.Y.H., 0000-0002-8914-139X

The sea urchin larva has been demonstrated to display bacteria in its digestive system (Schuh et al., 2020) and exhibit a specific microbial composition that correlates with its phenotype driven by environmental factors (Carrier and Reitzel, 2019a,b). Apparently, control of a specific larval microbiome is supported by the presence of a well-developed innate immune system in the sea urchin embryo. Infection of sea urchin larvae with the marine bacterium *Vibrio diazotrophicus* elicits an inflammatory response of the gut (Ho et al., 2016). During the inflammatory response, immune cells located in the ectoderm are activated and accumulate at the larval gut surface to phagocytose bacteria that leave the lumen through the midgut epithelium. Based on this observation and having insects and vertebrates as guiding examples, we formulate the hypothesis that the alkaline gut of the sea urchin larva may serve as a first barrier of defense to protect from environmental pathogens. In a first step, we determined pH-optimum curves for five species of marine bacteria to characterize their reproduction rate under alkaline midgut conditions. Secondly, we tested the physiological response of the midgut pH to *V. diazotrophicus* infections and studied the virulence of this bacterium during pharmacological inhibition of midgut alkalization. Finally, simulated OA conditions were used to assess the impact of this environmental stressor on the midgut pH homeostasis and the associated changes in resilience to a *V. diazotrophicus* infection.

MATERIALS AND METHODS

Bacteria cultures and pH optimum curves

Five species of bacteria were tested in this work with respect to their pH optimum. The species included *Vibrio diazotrophicus* (DSMZ 2064), *V. anguillarum* (DSMZ 11323), *V. alginolyticus* (DSMZ 2171) and *Planococcus citreus* (DSMZ 20549), which were all obtained from the German collection of microorganisms and cell cultures GmbH (DSMZ). *Salinibacterium amurskyense* (y338, KF306352.1 99%) was isolated from natural seawater (kindly provided by Dr Ruth Schmitz-Streit, University of Kiel). All bacteria were cultured in *Vibrio* medium composed of 10 g Tryptone, 10 g NaCl, 4 g $\text{MgCl}_2 \cdot 6 \text{H}_2\text{O}$ and 1 g KCl dissolved in 1 liter filtered sterilized distilled water. The media were autoclaved and pH was adjusted by the addition of HCl or NaOH to various pH values between 5.0 and 9.0. Cultures (15 ml) were inoculated with 10 μl of the respective bacteria stock solution and maintained at 22°C for the three *Vibrio* species or 30°C for *P. citreus* and *S. amurskyense* using a temperature-controlled incubator (INNOVA 40R, New Brunswick Scientific, Edison, NJ, USA). During the incubation period, the pH was continuously monitored using a pH meter (WTW, Weilheim, Germany, equipped with a sen Tix 81/MIC pH electrode). Optical densities were

monitored photometrically at 600 nm (OD600) using a Photometer (Ultraspec 1100pro, Amersham Biosciences, Cambridge, UK). Bacterial cultures were diluted to obtain a starting OD600 in the range of 0.03 to 0.07, which corresponded to a bacteria density of 1.2×10^6 to 6×10^7 cells ml^{-1} . Negative controls for background readings were prepared by omitting the addition of bacteria into the medium. For the determination of growth rates, OD600 was determined every 30 min during an incubation period of 3 h. All pH experiments with bacteria were performed in three to four biological replicates.

Sea urchin larval cultures and pH-perturbation experiments

Purple sea urchins (*Strongylocentrotus purpuratus*) were collected from the coast of California, USA, and transferred to the Helmholtz Centre for Ocean Research Kiel (GEOMAR), Kiel, Germany. The animals were maintained at 10°C in a 1000 liter recirculating seawater system inside a climate chamber. Animals were fed with *Laminaria* spp. and one-quarter of the seawater was changed three times per week. To obtain embryos, spawning was induced by gentle shaking of the adults, and eggs and sperm were collected for fertilization. The fertilized embryos were distributed into flasks filled with filtered seawater (15°C, salinity of 33). After 4 days post-fertilization (dpf), larvae were fed daily with *Rhodomonas* spp. (4000 cells ml^{-1}). pH/ P_{CO_2} perturbation experiments were performed as previously described (Stumpp et al., 2011; Hu et al., 2017). Briefly, the pH in the culture flasks was regulated by a computer-controlled system (pH controller, Aquamedic) that regulates the pH (NBS scale) by addition of pure gaseous CO_2 into the seawater (± 0.02 pH units). Water pH_{NBS}, salinity and temperature were monitored daily during the incubation period. Seawater samples for the determination of total alkalinity (A_T) were collected weekly and measured according to Sarazin et al. (1999). Seawater carbonate system speciation was calculated based on measured pH_{NBS} and alkalinity using the open-source program CO2SYS. Seawater physicochemical parameters measured during the experimental periods are summarized in Table 1.

Vibrio diazotrophicus infection experiments

For *V. diazotrophicus* infection experiments, 70 ml bottles were filled with 0.2 $\mu\text{mol l}^{-1}$ filtered seawater inoculated with bacteria to reach an OD600 corresponding to the required final bacteria concentration. Control larvae (3–7 dpf) or larvae from the pH perturbation experiments (3–12 dpf) were concentrated by mild centrifugation (5500 rpm, 1.7 g) and added to the experimental vials with a final concentration of 15 larvae ml^{-1} .

For gastric pH measurements, larvae were sampled from the infection vessels ($n=3$ per bacteria concentration) to monitor

Table 1. Physico-chemical seawater parameters of the two seawater acidification experiments

	Measured			Calculated		
	Temperature (°C)	Salinity	pH _{NBS}	A_T ($\mu\text{mol kg}^{-1}$ seawater)	P_{CO_2} (μatm)	C_T ($\mu\text{mol kg}^{-1}$ seawater)
Experiment 1	17.3 \pm 0.4	32	8.08 \pm 0.08	2305 \pm 29	375 \pm 81	2062 \pm 137
Pigment cell response & morphometry	17.3 \pm 0.4	32	7.92 \pm 0.02	2327 \pm 25	581 \pm 33	2124 \pm 129
	17.3 \pm 0.4	32	7.71 \pm 0.02	2241 \pm 29	939 \pm 34	2188 \pm 124
	17.3 \pm 0.4	32	7.51 \pm 0.02	2257 \pm 25	1546 \pm 74	2247 \pm 132
	17.3 \pm 0.4	32	7.31 \pm 0.02	2290 \pm 26	2539 \pm 103	2313 \pm 127
	17.3 \pm 0.4	32	7.22 \pm 0.03	2239 \pm 27	3087 \pm 225	2350 \pm 142
Experiment 2	17.2 \pm 0.03	32	8.07 \pm 0.03	2156 \pm 23	510 \pm 12	1967 \pm 47
Midgut pH	17.2 \pm 0.02	32	7.68 \pm 0.03	2231 \pm 78	1248 \pm 130	2185 \pm 67
	17.2 \pm 0.02	32	7.42 \pm 0.02	2144 \pm 83	2813 \pm 182	2203 \pm 90

A_T , total alkalinity; P_{CO_2} , partial pressure of CO_2 ; C_T , total dissolved inorganic carbon.

changes in midgut pH for the period of 30 h. In addition, one set of samples was collected at 12 h post-infection for gene expression analyses. A similar experiment was performed with the addition of different concentrations of 5-*n*-ethyl-isopropyl-amiloride (EIPA; specific inhibitor for Na⁺/H⁺ exchangers) using DMSO as a vehicle to test the virulence of *V. diazotrophicus* during inhibition of midgut alkalization. Larvae from the pH-perturbation experiments consisting of three replicates per pH treatment were sampled from the culture flasks, concentrated and added to the 70 ml infection vessels adjusted to the respective pH condition. Here as well, the final concentration of larvae in the infection vessels was 15 larvae ml⁻¹. The vessels were closed air-free to guarantee stability of the pH/*P*_{CO₂} and were put on a roller incubator at 17°C for 24 h. After this incubation time larval densities were measured and larvae were concentrated and fixed in 4% paraformaldehyde containing seawater (experiment 1). Pictures of the fixed larvae were taken under a microscope with AxioVision (Carl Zeiss Microscopy GmbH, Germany), and ImageJ (Version 1.51, National Institutes of Health, USA) was used to analyze larval morphology. Another experiment (experiment 2) was performed in a similar manner, but with three pH treatments only (pH 8.1, 7.7 and 7.4; *n*=3), to monitor midgut pH along a 6 h period of *Vibrio* infection with 10⁸ bacterial cells ml⁻¹. Pigment cells were regarded as 'activated' once a rounded shape had been observed.

Midgut pH measurements

Midgut pH of the larvae was measured following the method described previously (Stumpp et al., 2013, 2015) using H⁺-selective microelectrodes. Briefly, H⁺-selective microelectrodes with tip diameters of 2–3 μm were front loaded with a H⁺ ionophore (H⁺ ionophore III, Sigma-Aldrich) and back-filled with a KCl-based electrolyte (300 mmol l⁻¹ KCl, 50 mmol l⁻¹ NaPO₄, pH 7.0). The Nernstian potential generated by 1 pH unit was >52 mV. Gastric pH measurements were performed on an inverted microscope equipped with a cooling stage (10°C). Larvae were held in place with a holding pipette, to which a weak vacuum was applied. The H⁺ microelectrode was gently inserted through the esophagus (foregut) into the midgut. To test the effects of the Na⁺/H⁺-exchange inhibitor EIPA on midgut alkalization, larvae were incubated in seawater containing the respective concentration of the inhibitor dissolved in DMSO for 30 min and subsequently gastric pH was measured as described above. Control larvae were incubated in seawater containing 0.01% of the vehicle DMSO and served as the 0 mmol l⁻¹ EIPA group.

qPCR of midgut acid–base transporters

Transcriptional profiling of midgut acid–base transporter genes was performed as previously described (Lee et al., 2019). Briefly, after infection with *V. diazotrophicus* (10⁸ cells ml⁻¹) for 12 h, 3000–4000 larvae were concentrated by mild centrifugation (30 s, 1.7 g) using a table-top centrifuge. Seawater was removed and samples were flash-frozen in liquid nitrogen and stored at –80°C. Larval pellets were homogenized in TriZol and mRNA from the larvae was extracted using the Direct-zol™ RNA Micro/MiniPrep kit. DNA contamination was removed by DNase I treatment and cDNA was synthesized as described previously (Lee et al., 2019). Transcript levels of the target genes were quantified by qPCR using the LightCycler® 480 SYBR Green I Master (Roche). The target genes were three gastric acid–base transporters: Na⁺/K⁺-ATPase (*NKA*), Na⁺/H⁺-exchanger (*NHE*) and V-type H⁺-ATPase (*VHA*). After calculation of the ΔC_t value, transcript levels were normalized to *SP_Z12*, which has been demonstrated to be a stable housekeeping

gene in sea urchin embryos during early development (Hu et al., 2018; Lee et al., 2019). Primers used for qPCR analysis are listed in Lee et al. (2019).

Statistical analyses

Statistical analyses and graphical illustration were carried out using SigmaPlot Version 14.0. Significance levels for *post hoc* tests and *t*-tests were set to *P*=0.05 and *P*<0.001, respectively. One-way ANOVA followed by *post hoc* tests (Holm–Šidák method) was used to determine significant differences between *Vibrio* treatments in midgut pH and to determine the *Vibrio* effect on number of amoeboid cells. To compare regressions of infected versus uninfected larvae, one-way analysis of covariance (ANCOVA) followed by a *post hoc* test (Holm–Šidák) was performed. For testing the effect of *Vibrio* infection and seawater pH on stomach size, data were log transformed to obtain linear regressions. Student's *t*-test was performed to compare differences in gene expression levels of gastric acid–base transporters and between different EIPA treatments during *Vibrio* infection. All values are presented as means±s.e.m. and datasets were tested for normal distribution and homogeneity prior to statistical analyses.

Data repository

Data are available at PANGAEA – Data Publisher for Earth & Environmental Science under the identifier 914693.

RESULTS

Growth rates of marine bacteria under a wide range of seawater pH

For all bacteria species tested in this study, a growth optimum was found at an average seawater pH value of approximately 8.0. Depending on the species, a wider or narrower pH optimum plateau was observed. *Vibrio diazotrophicus* has the narrowest pH optimum, ranging from pH 7.5 to 8.0. Beyond this pH range, growth rates decrease rapidly down to 20% and 40% at pH 6.0 and 9.0, respectively (Fig. 1A). The widest pH optimum was determined for *S. amurskyense*, with average growth rates of 90% between pH 6.0 and 9.0. Beyond pH 9.0, all bacteria responded with substantial decreases in proliferation rates by 50–60%. Between pH 8.0 and 9.0, *V. diazotrophicus* revealed a linear relationship between proliferation rates and environmental pH (Fig. 1B). This linear relationship demonstrates a decrease in bacterial growth of 46%, when pH is increased by 1 pH unit representing pH conditions in the larval gut of sea urchins (pH 9.0).

Response of the midgut pH regulatory machinery during *Vibrio* infection

H⁺-selective microelectrodes were used to determine midgut pH conditions during an infection with *V. diazotrophicus*. In uninfected larvae, the midgut pH ranges from 9.0 to 9.15 (Fig. 2A). Upon infection with different concentrations of bacteria, midgut pH begins to fluctuate, ranging from 8.8 to 9.25. Highest fluctuations of up to 0.5 pH units were observed in larvae infected with 10⁸ bacteria cells ml⁻¹ within the first 10 h of infection. At later time points (up to 30 h), midgut pH fluctuations were less pronounced and reached control levels in larvae infected with 10⁶ and 10⁷ bacteria cells ml⁻¹. Transcript levels of the gastric acid–base transporters *NKA*, *VHA* and *NHE* were determined by qPCR. While expression of *VHA* remained unchanged during *Vibrio* infection, *NKA* and *NHE* responded significantly with a 2-fold and 42-fold increase in transcript levels, respectively (Fig. 2B).

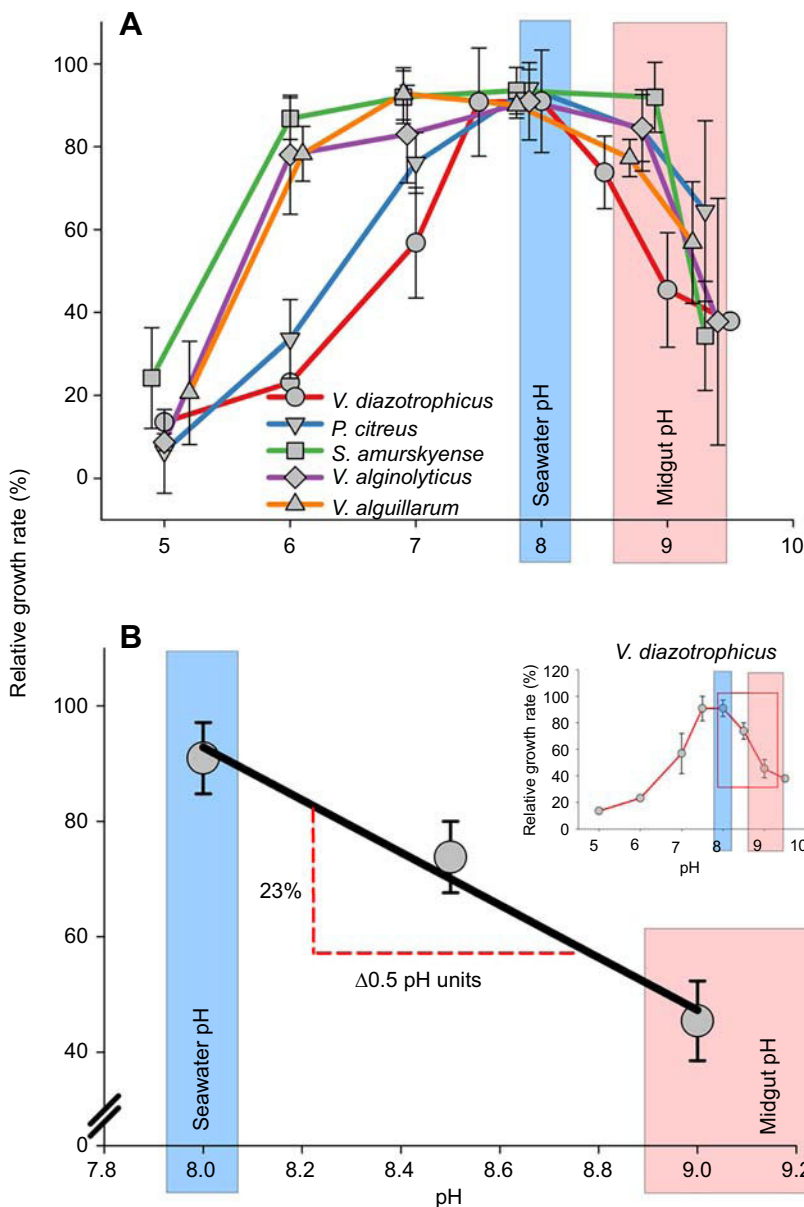


Fig. 1. Growth optima for five species of marine bacteria. (A) pH optimum curves were generated by cultivating bacteria (*Vibrio diazotrophicus*, *V. anguillarum*, *V. alginolyticus*, *Planococcus citreus* and *Salinibacterium amurskyense*) under a range of different pH conditions. Growth rates were determined by photometric density measurements and expressed as relative to the maximal growth rate observed within each strain. (B) Magnification of pH-dependent growth rate of *V. diazotrophicus* between pH 8.0 and 9.0 from A. In this pH range, an increase by 0.5 pH units decreases bacterial growth by 23%. Values are presented as means \pm s.e.m. ($n=3-4$).

Effect of pharmacological inhibition of midgut alkalization on immunity to *Vibrio*

Gastroscopic pH measurements in combination with the Na^+/H^+ -exchanger inhibitor EIPA demonstrated a dose-dependent reduction in midgut pH (Fig. 3A). A concentration of $5 \mu\text{mol l}^{-1}$ EIPA resulted in a maximum inhibition of midgut alkalization and the IC_{50} was $0.8 \mu\text{mol l}^{-1}$. *Vibrio diazotrophicus* were cultured under different EIPA concentrations to exclude a direct effect of EIPA on bacterial growth. These experiments demonstrated that this compound had no effect on bacterial growth up to a concentration of $20 \mu\text{mol l}^{-1}$ (Fig. 3B). To assess the effects of reduced midgut pH on larval immunity, larvae were infected with 10^8 bacteria ml^{-1} in the presence of different EIPA concentrations (Fig. 3C). Different EIPA concentrations in the presence of PFA-killed bacteria led to an increase in mortality rates with increasing EIPA concentration from $0.03 \text{ larvae h}^{-1}$ up to $0.15 \text{ larvae h}^{-1}$. However, larvae infected with live *Vibrio* bacteria demonstrated significantly increased mortality rates of 0.26 , 0.22 and $0.21 \text{ larvae h}^{-1}$ at EIPA concentrations of 2.5 , 5 and $10 \mu\text{mol l}^{-1}$, respectively. During

V. diazotrophicus infection, pigment cells from the ectoderm were activated and migrated towards the midgut epithelium (Fig. 4A). During a bacterial infection with 10^8 bacteria cells ml^{-1} , an average of 5.25 ± 0.75 rounded pigment cells were found at the stomach, whereas an average of 4.0 ± 0.9 remained at the ectoderm (Fig. 4A). In the presence of $2.5 \mu\text{mol l}^{-1}$ EIPA, the number of rounded pigment cells at the midgut dropped to 0.57 ± 0.2 during a *Vibrio* infection. However, the number of activated rounded pigment cells at the ectoderm was significantly increased to 8.4 ± 1.2 cells compared with control larvae. In the presence of PFA-killed bacteria, no differences in pigment cell activation and migration were observed in EIPA-treated larvae and the control.

Effects of seawater acidification on gastric pH homeostasis and pigment cell behavior upon infection

Acidified water induced a developmental delay and resulted in smaller larvae. However, the size (diameter) of the midgut increased relatively to the larval size, leading to an exponential increase in the midgut size/body length ratio from 22 to 27 with

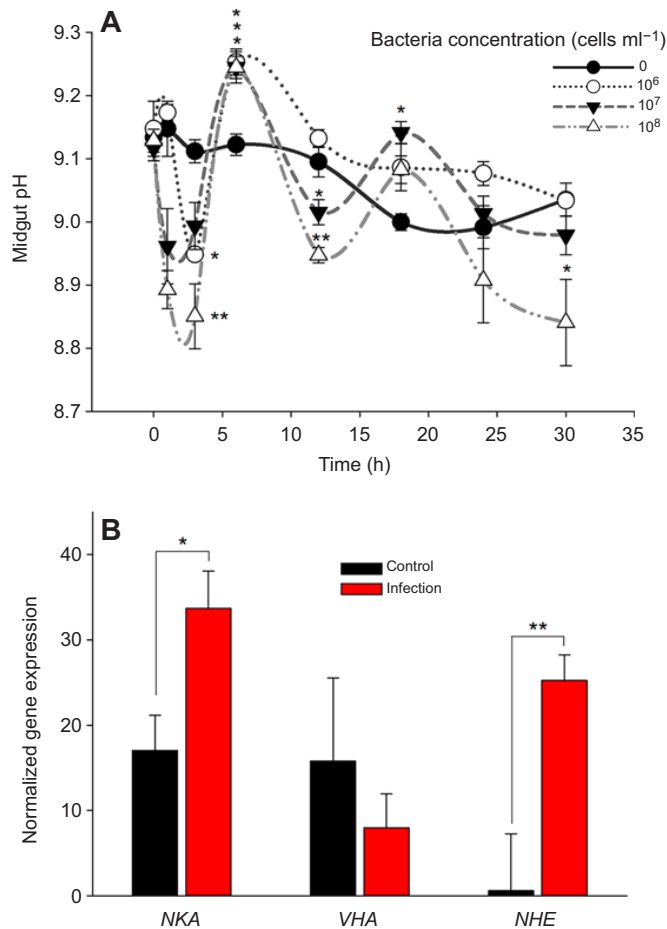


Fig. 2. Response of the midgut pH regulatory machinery during a *V. diazotrophicus* infection. (A) Midgut pH measurements using H⁺-selective microelectrodes were performed in sea urchin larvae along a 30 h infection period with different concentrations of *V. diazotrophicus* ($n=5$, ANOVA). (B) Transcript levels of three midgut acid–base transporters were determined using RT-qPCR after an infection period of 12 h with a bacterial load of 10^8 bacterial cells per ml. Gene expression levels were normalized to the housekeeping gene *SP_Z12*. Values are presented as means \pm s.e.m. ($n=4$). Asterisks denote significant differences: * $P<0.05$, ** $P<0.001$ (t -test).

decreasing seawater pH (Fig. 5A). Larvae infected with 5×10^8 bacterial cells ml⁻¹ had an overall reduction in midgut size, resulting in a downward shift in the regression curve (ANCOVA, $F_{1,32}=47.8$, $P<0.001$; Holm–Šidák, $t=116.4$, $P<0.001$; intercept). In uninfected larvae, the number of activated (rounded) pigment cells attached at the midgut was low (ca. 0–2 cells per larva) and not affected by seawater pH. However, during a *Vibrio* infection, the number of activated pigment cells increased to 13.5 ± 0.4 at pH 8.1, leading to a significant difference between the intercept of the regressions of infected and uninfected larvae (ANCOVA, $F_{1,29}=148.1$, $P<0.001$; Holm–Šidák, $t=12.2$, $P<0.001$). In addition, the number of activated pigment cells during a *Vibrio* infection was significantly affected by reductions in seawater pH that resulted in a decreased number of activated pigment cells down to an average of 8.2 ± 1.6 cells per larva at pH 7.2 (Fig. 5B). Survival indicated by larval density was decreased under acidified conditions, but was not affected by the bacteria treatment (Fig. 5C). Using H⁺-selective microelectrodes, we demonstrated that midgut pH was decreased under acidified conditions, with gastric pH values of 8.62 ± 0.03 and 8.38 ± 0.14 (at seawater pH of 7.7 and 7.4, respectively) compared

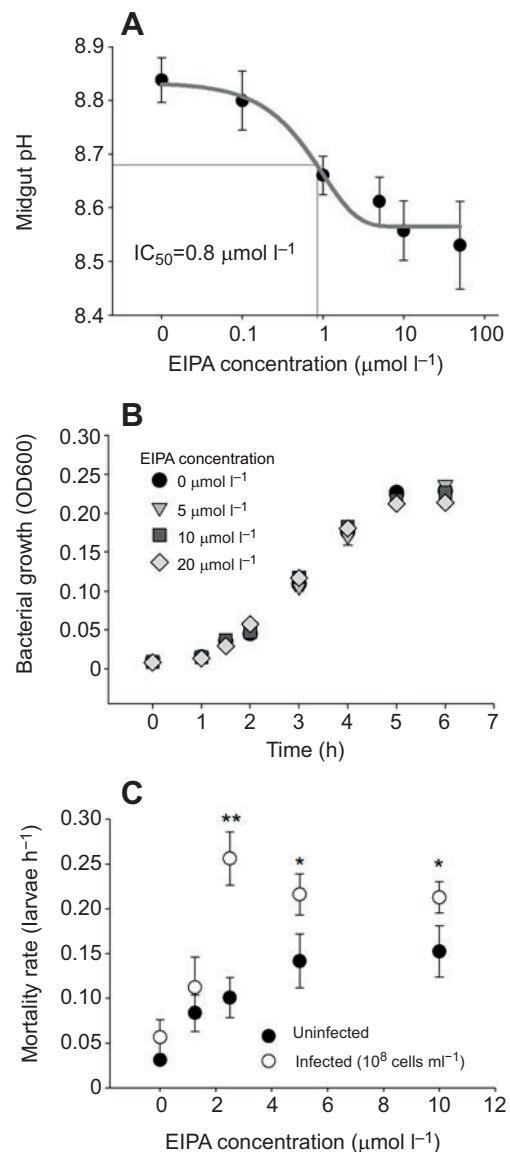


Fig. 3. Effect of inhibited midgut alkalization on larval mortality during *V. diazotrophicus* infection. (A) Dose–response curve for the inhibition of midgut alkalization by EIPA, a specific inhibitor for Na⁺/H⁺ exchangers. (B) Bacterial growth remained unaffected by different concentrations of EIPA. (C) Mortality rates of larvae at several time points (1, 2.5, 18 and 23 h) in the presence of five different EIPA concentrations in combination with *V. diazotrophicus* infections (10^8 cells ml⁻¹). Values are presented as means \pm s.e.m. ($n=4$). Asterisks denote significant differences: * $P<0.05$, ** $P<0.001$ (ANOVA).

with the control seawater condition of pH 8.1 with a gastric pH of 8.93 ± 0.11 (Fig. 6A). Larvae raised at pH 8.1 significantly increased the midgut pH after 6 h of *V. diazotrophicus* infection by 0.20 ± 0.02 pH units (Fig. 6B). Although no significant differences were detected in the moderate acidification level of pH 7.7, substantial increases in midgut pH by 0.40 ± 0.13 and 0.39 ± 0.13 were measured at the infection time points of 4 and 6 h, respectively, in the pH 7.4 treatment (Fig. 6B).

DISCUSSION

Distinct pH conditions are a requisite of all digestive systems in the animal kingdom. The pH homeostasis is critical for the breakdown of ingested food by digestive enzymes (Piper and Fenton, 1965;

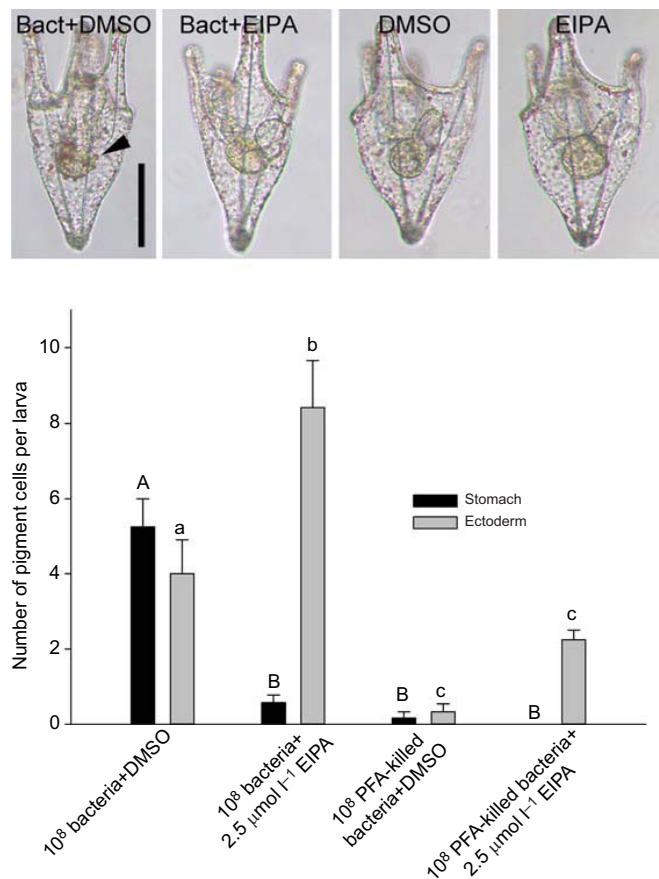


Fig. 4. Effects of EIPA on the immune response of phagocytotic cells during *Vibrio* infection. Light microscopic images of larvae infected with 10^8 bacteria ml^{-1} in the presence or absence of EIPA. The arrowhead indicates accumulation of rounded pigment cells at the midgut (upper panel). Effects of EIPA and of *V. diazotrophicus* infection on the number of rounded pigment cells located at the ectoderm and midgut epithelial cell. Values are presented as means \pm s.e.m. ($n=4$). Letters denote significant differences between the amount of rounded pigment cells at the ectoderm (lowercase letters) and midgut (uppercase letters) ($P<0.05$, ANOVA). Scale bar: 100 μm .

Solovyev et al., 2015) and helps to maintain a healthy gut microbiota (Beasley et al., 2015). This work tested the hypothesis that alkaline conditions in the midgut of the sea urchin larva may represent a physiological trait that helps to protect it from environmental pathogens. Using the sea urchin larva as a model, a set of experiments were performed to investigate the effects of CO_2 -induced seawater acidification on midgut pH homeostasis and the associated changes in larval immunity.

Response of the midgut pH homeostasis during bacterial infection

The pH optima for the growth of five species of marine bacteria were determined demonstrating highest growth rates for all species at average seawater pH conditions found in the open ocean, i.e. pH 8.0. Although some bacteria have a higher tolerance towards acidic conditions than others, all species tested showed substantial reductions in proliferation rates at pH conditions $>\text{pH } 9.0$. This pH optimum is presumably a result of a long-term adaptation to very constant pH conditions in the range of pH 8 over long evolutionary time scales (Zeebe, 2012). A higher tolerance towards more acidic conditions, i.e. pH 6–7, may have derived from naturally acidified habitats including benthic ecosystems or upwelling regions (Feely

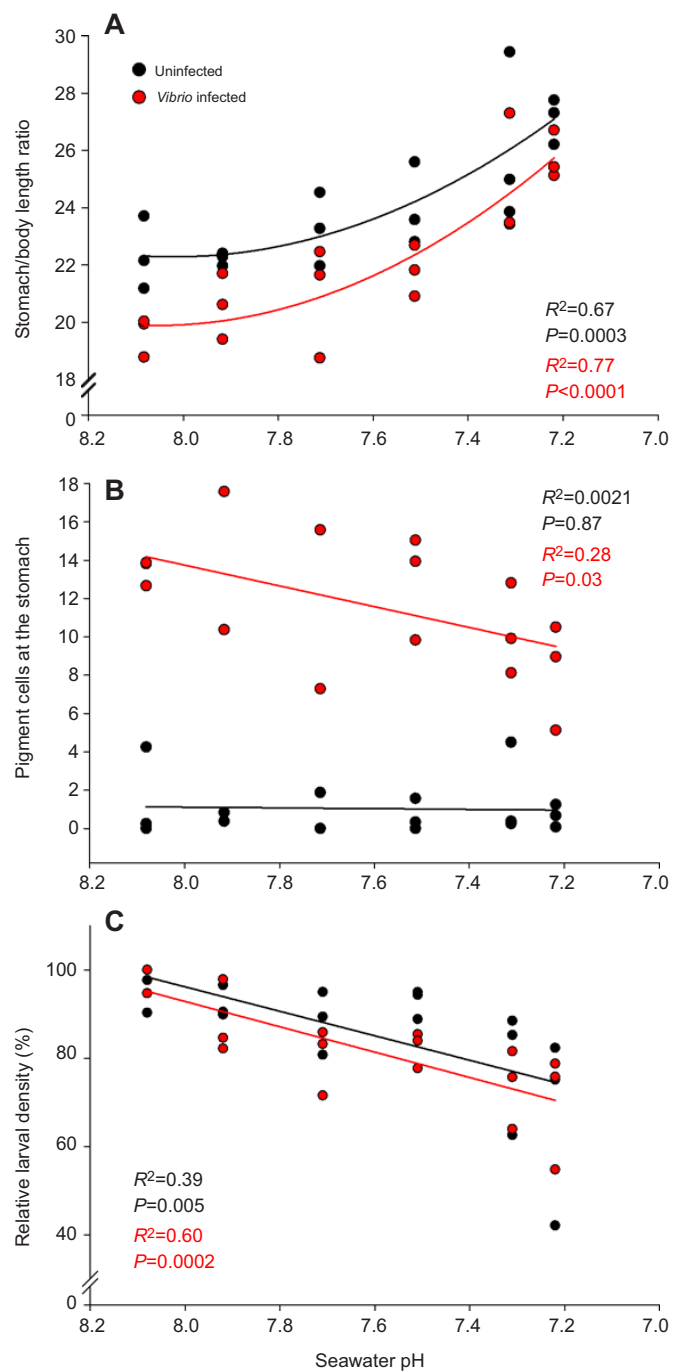


Fig. 5. Stomach morphometry and immune response and mortality under a wide range of seawater pH and *Vibrio* infection. (A) The ratio between midgut diameter and body length was used as an indicator for changes in the stomach morphology during a 24 h bacterial infection (10^8 cells ml^{-1}) normalized to the reductions in body size derived from the exposure to acidified conditions. Black, uninfected; red, infected. (B) Number of activated (rounded) pigment cells that are associated with the stomach were determined for infected and uninfected larvae raised under different pH regimes. (C) Larval densities were determined after the infection period in relation to the starting time point (24 h) in infected and uninfected larvae to determine the mortality as a function of seawater pH ($P<0.05$, $n=3$, ANCOVA).

et al., 2008; Melzner et al., 2013). However, conditions more alkaline than pH 8.5 are very rarely seen in the marine environment and are mainly associated with hydrothermal vent systems (Kelly et al., 2001; Shibuya et al., 2010; Zeebe, 2012). The typical pH of

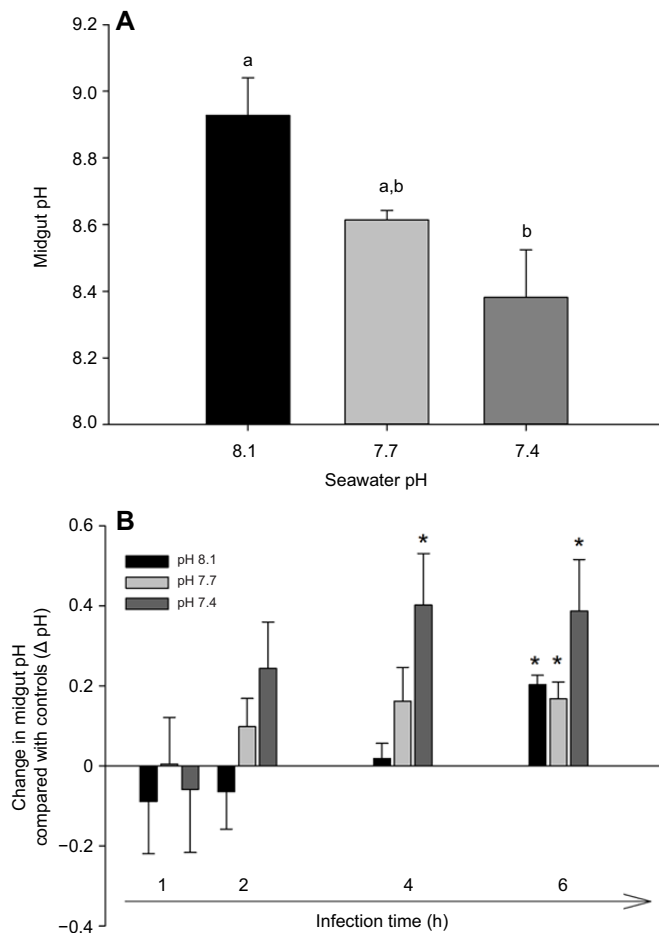


Fig. 6. Midgut pH under different pH conditions and after *V. diazotrophicus* infection. (A) Midgut pH of sea urchin larvae was measured using H^+ selective microelectrodes and demonstrated a drop in pH during exposure to acidified conditions. (B) Sea urchin larvae raised under the three different pH regimes indicated responded with changes in midgut pH during a 6 h *V. diazotrophicus* infection period with 10^8 cells ml^{-1} . Values are presented as means \pm s.e.m. ($n=3$). Asterisks denote significant differences between pH treatments: * $P<0.05$, ANOVA.

the marine environment may explain the relatively uniform reduction in proliferation of marine bacteria at pH values exceeding pH 8.5.

The midgut pH of the sea urchin larva that is in the range of pH 8.8 to 9.5 (Stumpp et al., 2015; Hu et al., 2017) is clearly beyond the growth optimum of the five bacteria species tested in this work. Accordingly, pH conditions in the larval gut can decrease bacterial growth by up to 60% compared with larvae growing under pH conditions of the marine environment. This potential selection mechanism is underlined by a sharp decrease in bacterial abundance and diversity of the larval microbiome when the alkaline gut has developed and feeding begins (Carrier and Reitzel, 2019b). Furthermore, analyses of bacterial communities along the larval development of three echinoid species demonstrated that their microbiome is primarily dominated by α - and γ -proteobacteria after the functional development of the gut (Carrier and Reitzel, 2019b) and bacteria are mostly associated with the digestive system (Schuh et al., 2020).

During infection of the gut by *V. diazotrophicus* over a period of 30 h, midgut pH homeostasis shows dynamic fluctuations when

compared with uninfected larvae. These fluctuations begin within a few hours after infection and include reductions as well as increases in midgut pH by up to 0.2 and 0.15 pH units, respectively. These alterations in midgut pH homeostasis are accompanied by increased expression of key genes coding for midgut acid–base transporters at the time point of 6 h post-infection. Previous studies addressing the immune response of the sea urchin larva to a *V. diazotrophicus* infection demonstrated an onset of the cellular immune response within 6 h (e.g. Ho et al., 2016). At this time point, increases in the expression level of other gut-related genes including *Sou11*, *IL-17-4* and *IL-17-1* have been observed in response to a *Vibrio* infection, followed by a progressive decrease in expression levels over the time course of 24 h (Buckley and Rast, 2019). The relative synchrony of the cellular immune response with changes in midgut pH homeostasis after *Vibrio* infection suggests an orchestration of these systems in response to a bacterial infection of the gut.

To address the physiological significance of the highly alkaline midgut pH on the resilience of the sea urchin larva to environmental pathogens, we pharmacologically inhibited midgut alkalization. Increased mortality during challenge with *V. diazotrophicus* was observed in larvae with impaired midgut alkalization suggesting that the alkaline conditions in the gut are associated with a lower susceptibility of larvae to infection. The immune response of the sea urchin larva during *V. diazotrophicus* infection of the gut has been described to include a coordinated activation and migration of immune cells (pigment cells) towards the midgut (Ho et al., 2016). Here, pigment cells migrated from the epidermis to the stomach epithelium and phagocytosed bacteria that migrate from the lumen of the gut into the blastocoel. These findings are in accordance with observations of the present work in that infection of the larvae with *V. diazotrophicus* stimulated pigment cells to migrate to the stomach. Inhibition of gastric alkalization using the NHE inhibitor EIPA also affected the migration behavior of pigment cells by significantly reducing the number of pigment cells located at the stomach during infection. Although it is likely that gastric alkalization and the activation and migration of pigment cells are linked to innate immune responses, we cannot exclude the direct effect of the inhibitor on immune cell function. For example, NHE proteins were described to play a central role in generating sub-cellular pH gradients that are required for directional movement of keratinocytes (Bereiter-Hahn and Vöth, 1988), leukocytes (Simchowicz and Cragoe, 1986; Ritter et al., 1998) such as neutrophil granulocytes (Rosengren et al., 1994), and fibroblasts (Denker and Barber, 2002). Thus, it remains a future task to dissect the roles of intestine pH homeostasis and of immune cell activation in the defense reaction of the sea urchin larva towards bacterial infection of the midgut.

Gut pH homeostasis and pathogen defense under acidified seawater conditions

The present work confirmed that of previous studies (Stumpp et al., 2013; Lee et al., 2019) in that reductions in seawater pH in the context of anthropogenic-driven OA reduced the midgut pH in the sea urchin larva. This observation has led to the hypothesis that reductions in seawater pH may also affect the tolerance of the sea urchin larva during bacterial infection of the gut. In accordance with observations made by others (Ho et al., 2016), infection of the gut by *V. diazotrophicus* affects the morphology of the midgut with a smaller inner and outer diameter as well as a thicker midgut epithelium. These changes in midgut morphology are reflected in a

decreased midgut/body length ratio. This ratio was generally increased by reductions in seawater pH without *Vibrio* infection, indicating a maintained midgut size despite a decreased growth of the larval body. The number of pigment cells located at the stomach during *Vibrio* infection was significantly decreased under acidified conditions, supporting the hypothesis of an interaction between midgut alkalization and the cellular immune response in the blastocoel. Finally, the combined effects of *Vibrio* infection and reductions in seawater pH had no effect on the mortality of sea urchin larvae, suggesting compensatory mechanisms of midgut pH homeostasis to be in place.

Interestingly, larvae that were exposed to the lowest pH treatment, i.e. pH 7.4, fully restored their gut pH from initially pH 8.4 to 8.8 during infection with *V. diazotrophicus*. This stimulation of midgut alkalization indicates a necessity of the larvae to elevate pH conditions during *Vibrio* infection. Together with our inhibitor experiments that demonstrated increased mortality during *Vibrio* infection when midgut alkalization was impaired, one may conclude that midgut alkalization plays a critical role during infection with this bacterium. Maintenance of an alkaline midgut is achieved by a set of acid–base transporters that depend on the electrochemical gradient of the Na^+/K^+ -ATPase (Stumpp et al., 2015). Consequently, stimulation of the midgut acid–base regulatory machinery to compensate for long-term environmentally induced reductions in midgut pH in combination with bacterial infections will add an additional energetic challenge to the larva. In this experiment, no changes in mortality under different pH conditions were measured, probably because of the relatively short exposure time of 24 h. Thus, longer exposure times in combination with changes in ambient pH are necessary to push the larvae beyond their energetic limits, which may lead to increased mortality by the combined stressors of bacterial infection and seawater acidification.

Conclusions

To the best of our knowledge, this is the first study that addresses the role of the alkaline gut of echinoderm larvae as a first line of immunity. The importance of this physiological trait is reflected in the evolution of highly alkaline larval guts in all Ambulacraria (echinoderms and hemichordates) species tested so far, including sea urchins, brittle stars, sea stars and acorn worms (Hu et al., 2017). The extreme pH conditions up to pH 10.5 can be regarded as a strong selection factor to control the larval gut microbiome. In fact, distinct microbial compositions were associated with different developmental stages of the sea urchin larva, with a strong decrease in bacterial diversity and abundance in larvae after the development of the functional gut (Carrier and Reitzel, 2019b). In addition, the larval gut appears to represent an important site for the coordination of a cellular immune response during bacterial infections (Buckley and Rast, 2019). These observations strongly suggest a concerted action of cellular immune responses and midgut pH in regulating the larval microbiome.

Sea urchin larvae were shown to be capable of compensating for intracellular and extracellular pH homeostasis and biochemical processes with an increased energy expenditure when exposed to reductions in seawater pH predicted for the coming century (Stumpp et al., 2011; Pan et al., 2015; Lee et al., 2019). According to the present study, energetic allocations towards maintenance of midgut pH in the sea urchin larva might exceed their limits in future pelagic systems under the effects of acidification and bacterial infection. Because the larval physiology has been demonstrated to be intrinsically linked to seawater pH, this work provides a first insight into the complex interactions between environment, host

physiology and microbes which opens new important avenues for future research.

Acknowledgements

We thank J. Hildebrand for valuable help to maintain the sea urchin facility and S. Brandt for assistance in generating pH optimum curves for marine bacteria.

Competing interests

The authors declare no competing or financial interests.

Author contributions

Conceptualization: M.S., J.Y., M.L., M.Y.H.; Methodology: M.S., I.P., F.T., J.Y., M.L., M.Y.H.; Validation: M.S., I.P., F.T., M.Y.H.; Formal analysis: F.T.; Investigation: M.S., I.P., F.T., J.Y., M.Y.H.; Resources: M.S., M.L., M.Y.H.; Data curation: M.S.; Writing - original draft: M.S., M.Y.H.; Writing - review & editing: M.S., I.P., F.T., J.Y., M.L., M.Y.H.; Visualization: F.T., J.Y., M.Y.H.; Supervision: M.S., M.L., M.Y.H.; Funding acquisition: M.S., M.L., M.Y.H.

Funding

M.Y.H. was funded by the Emmy Noether Program (403529967) of the German Research Foundation (Deutsche Forschungsgemeinschaft). M.S. was funded through the Young Scientists Research grant by Kiel Life Sciences of the Christian-Albrechts-University of Kiel.

Data availability

Data are available at PANGAEA – Data Publisher for Earth & Environmental Science under the identifier 914693.

References

- Azuma, M., Harvey, W. R. and Wieczorek, H. (1995). Stoichiometry of K^+/H^+ antiport helps to explain extracellular pH 11 in a model epithelium. *FEBS Lett.* **361**, 153–156. doi:10.1016/0014-5793(95)00146-Z
- Beasley, D. E., Koltz, A. M., Lambert, J. E., Fierer, N. and Dunn, R. R. (2015). The evolution of stomach acidity and its relevance to the human microbiome. *PLoS ONE* **10**, e0134116. doi:10.1371/journal.pone.0134116
- Bereiter-Hahn, J. and Vöth, M. (1988). Ionic control of locomotion and shape of epithelial cells: II. Role of monovalent cations. *Cell Motil. Cytoskeleton* **10**, 528–536. doi:10.1002/cm.970100409
- Boudko, D. Y., Moroz, L. L., Harvey, W. R. and Linser, P. J. (2001). Alkalization by chloride/bicarbonate pathway in larval mosquito midgut. *Proc. Natl. Acad. Sci. USA* **98**, 15354–15359. doi:10.1073/pnas.261253998
- Brune, A. (1998). Termite guts: the world's smallest bioreactors. *Trends Biotechnol.* **16**, 16–21. doi:10.1016/S0167-7799(97)01151-7
- Brune, A. and Kühl, M. (1996). pH profiles of the extremely alkaline hindguts of soil-feeding termites (Isoptera: Termitidae) determined with microelectrodes. *J. Insect Physiol.* **42**, 1121–1127. doi:10.1016/S0022-1910(96)00036-4
- Buckley, K. M. and Rast, J. P. (2019). Immune activity at the gut epithelium in the larval sea urchin. *Cell Tissue Res.* **377**, 469–474. doi:10.1007/s00441-019-03095-7
- Carrier, T. J. and Reitzel, A. M. (2019a). Shift in bacterial taxa precedes morphological plasticity in a larval echinoid. *Marine Biol.* **166**, 164. doi:10.1101/640953
- Carrier, T. J. and Reitzel, A. M. (2019b). Bacterial community dynamics during embryonic and larval development of three confamilial echinoids. *Mar. Ecol. Prog. Ser.* **611**, 179–188. doi:10.3354/meps12872
- Denker, S. P. and Barber, D. L. (2002). Cell migration requires both ion translocation and cytoskeletal anchoring by the Na-H exchanger NHE1. *J. Cell Biol.* **159**, 1087–1096. doi:10.1083/jcb.200208050
- Feely, R. A., Sabine, C. L., Hernandez-Ayon, J. M., Jansson, D. and Hales, B. (2008). Evidence for upwelling of corrosive 'acidified' water onto the continental shelf. *Science* **320**, 1490–1492. doi:10.1126/science.1155676
- Hammer, T. J., Janzen, D. H., Hallwachs, W., Jaffe, S. P. and Fierer, N. (2017). Caterpillars lack a resident gut microbiome. *Proc. Natl. Acad. Sci. USA* **114**, 9641–9646. doi:10.1073/pnas.1707186114
- Ho, E. C., Buckley, K. M., Schrankel, C. S., Schuh, N. W., Hibino, T., Solek, C. M., Bae, K., Wang, G. and Rast, J. P. (2016). Perturbation of gut bacteria induces a coordinated cellular immune response in the purple sea urchin larva. *Immunol. Cell Biol.* **94**, 861–874. doi:10.1038/icb.2016.51
- Hu, M. Y., Tseng, Y.-C., Su, Y.-H., Lin, E., Lee, H.-G., Lee, J.-R., Dupont, S. and Stumpp, M. (2017). Variability in larval gut pH regulation defines sensitivity to ocean acidification in six species of the Ambulacraria superphylum. *Proc. R. Soc. Lond. B* **284**, 20171066. doi:10.1098/rspb.2017.1066
- Hu, M. Y., Yan, J.-J., Petersen, I., Himmerkus, N., Bleich, M. and Stumpp, M. (2018). A Slc4 family bicarbonate transporter is critical for intracellular pH regulation and biomineralization in sea urchin embryos. *elife* **7**, e36600. doi:10.7554/eLife.36600

- Jaskiewicz, K., Van Helden, P. D., Wiid, I. J., Steenkamp, H. J. and Van Wyk, M. J. (1990). Chronic atrophic gastritis, gastric pH, nitrites and micronutrient levels in a population at risk for gastric carcinoma. *Anticancer Res.* **10**, 833-836.
- Kelly, D. S., Karson, J. A., Blackman, D. K., Früh-Green, G. L., Butterfield, D. A., Lilley, M. D., Olson, E. J., Schrenk, M. O., Roe, K. K., Lebon, G. T. et al. (2001). An off-axis hydrothermal vent field near the Mid-Atlantic Ridge at 30°N. *Nature* **412**, 145-149. doi:10.1038/35084000
- Koelz, H. R. (1992). Gastric acid in vertebrates. *Scand. J. Gastroenterol.* **27**, 2-6. doi:10.3109/00365529209095998
- Lee, H.-G., Stumpp, M., Yan, J.-J., Tseng, Y.-C., Heinzel, S. and Hu, M. Y.-A. (2019). Tipping points of gastric pH regulation and energetics in the sea urchin larva exposed to CO₂-induced seawater acidification. *Comp. Biochem. Physiol. A* **234**, 87-97. doi:10.1016/j.cbpa.2019.04.018
- Melzner, F., Thomsen, J., Koeve, W., Oschlies, A., Gutowska, M. A., Bange, H. W., Hansen, H. P. and Körtzinger, A. (2013). Future ocean acidification will be amplified by hypoxia in coastal habitats. *Mar. Biol.* **160**, 1875-1888. doi:10.1007/s00227-012-1954-1
- Pan, T.-C. F., Applebaum, S. L. and Manahan, D. T. (2015). Experimental ocean acidification alters the allocation of metabolic energy. *Proc. Natl. Acad. Sci. USA* **112**, 4696-4701. doi:10.1073/pnas.1416967112
- Piper, D. W. and Fenton, B. H. (1965). pH stability and activity curves of pepsin with special reference to their clinical importance. *Gut* **6**, 506-508. doi:10.1136/gut.6.5.506
- Ritter, M., Schratzberger, P., Rossmann, H., Wöll, E., Seiler, K., Seidler, U., Reinisch, N., Kähler, C. M., Zwierzina, H., Lang, H. J. et al. (1998). Effect of inhibitors of Na⁺/H⁺-exchange and gastric H⁺/K⁺ ATPase on cell volume, intracellular pH and migration of human polymorphonuclear leucocytes. *Br. J. Pharmacol.* **124**, 627-638. doi:10.1038/sj.bjp.0701864
- Rosengren, S., Henson, P. M. and Worthen, G. S. (1994). Migration-associated volume changes in neutrophils facilitate the migratory process in vitro. *Am. J. Physiol.* **267**, C1623-C1632. doi:10.1152/ajpcell.1994.267.6.C1623
- Sarazin, G., Michard, G. and Prevot, F. (1999). A rapid and accurate spectroscopic method for alkalinity measurements in sea water samples. *Water Res.* **33**, 290-294. doi:10.1016/S0043-1354(98)00168-7
- Schuh, N. W., Carrier, T. J., Schrankel, C. S., Reitzel, A. M., Heyland, A. and Rast, J. P. (2020). Bacterial exposure mediates developmental plasticity and resistance to lethal *Vibrio lentus* infection in purple sea urchin (*Strongylocentrotus purpuratus*) larvae. *Front. Immunol.* **10**, 3014. doi:10.3389/fimmu.2019.03014
- Shibuya, T., Komiya, T., Nakamura, K., Takai, K. and Maruyama, S. (2010). Highly alkaline, high-temperature hydrothermal fluids in the early Archean ocean. *Precamb. Res.* **182**, 230-238. doi:10.1016/j.precamres.2010.08.011
- Simchowitz, L. and Cragoe, E. J. J. (1986). Regulation of human neutrophil chemotaxis by intracellular pH. *J. Biol. Chem.* **261**, 5492-5500.
- Smith, J. L. (2003). The role of gastric acid in preventing foodborne disease and how bacteria overcome acid conditions. *J. Food Prot.* **7**, 1115-1325. doi:10.4315/0362-028X-66.7.1292
- Solovyev, M. M., Kashinskaya, E. N., Izvekova, G. I. and Glupov, V. V. (2015). pH values and activity of digestive enzymes in the gastrointestinal tract of fish in Lake Chany (West Siberia). *J. Ichthyol.* **55**, 251-258. doi:10.1134/S0032945215010208
- Stumpp, M., Wren, J., Melzner, F., Thorndyke, M. C. and Dupont, S. T. (2011). CO₂ induced seawater acidification impacts sea urchin larval development I: elevated metabolic rates decrease scope for growth and induce developmental delay. *Comp. Biochem. Physiol. A* **160**, 331-340. doi:10.1016/j.cbpa.2011.06.022
- Stumpp, M., Hu, M., Casties, I., Saborowski, R., Bleich, M., Melzner, F. and Dupont, S. (2013). Digestion in sea urchin larvae impaired under ocean acidification. *Nat. Climate Change* **3**, 1044-1049. doi:10.1038/nclimate2028
- Stumpp, M., Hu, M. Y., Tseng, Y.-C., Guh, Y.-J., Chen, Y.-C., Yu, J.-K., Su, Y.-H. and Hwang, P.-P. (2015). Evolution of extreme stomach pH in Bilateria inferred from gastric alkalization mechanisms in basal deuterostomes. *Sci. Rep.* **5**, 10421. doi:10.1038/srep10421
- Tennant, S. M., Hartland, E. L., Phumoonna, T., Lyras, D., Rood, J. L., Robins-Browne, R. M. and van Driel, I. R. (2008). Influence of gastric acid on susceptibility to infection with ingested bacterial pathogens. *Infect. Immun.* **76**, 639-645. doi:10.1128/IAI.01138-07
- Zeebe, R. E. (2012). History of seawater carbonate chemistry, atmospheric CO₂ and ocean acidification. *Annu. Rev. Earth Planet. Sci.* **40**, 141-165. doi:10.1146/annurev-earth-042711-105521